Progress In Electromagnetics Research Letters, Vol. 46, 25–30, 2014

Dual-Band Dual-Polarized Spiral Antenna for Chinese Compass Navigation Satellite System

Hangying Yuan[1, *], Shaobo Qu[1], Jieqiu Zhang[1], Hang Zhou[1], Jiafu Wang[1], Hua Ma[1], and Zhuo Xu[2]

Abstract—In Chinese Compass Navigation Satellite System (CNSS for short), dual-band antennas are more attractive, because they can provide both navigation and communication services. In this paper, we present a dual-band dual-circular-polarized planar spiral-slot CNSS antenna. This antenna works at L band (1616 ± 5 MHz, left-handed circular polarization, LHCP) and S band (2492 ± 5 MHz, right-handed circular polarization, RHCP). Numerical results show that the impedance bandwidth ($S_{11} < -10$ dB), 3 dB axial ratio bandwidth and antenna gain at L band are about 242 MHz, 79 MHz and 4.92 dB, respectively, while the simulated impedance bandwidth ($S_{11} < -10$ dB), 3 dB axial ratio bandwidth and antenna gain at S band are about 180 MHz, 58 MHz and 5.25 dB, respectively. An experiment was carried out to verify our design. Measured results show that impedance bandwidth ($S_{11} < -10$ dB) and 3 dB axial ratio bandwidth L band are about 300 MHz and 14 MHz, respectively, while the measured impedance bandwidth ($S_{11} < -10$ dB) and 3 dB axial ratio bandwidth at S band are about 210 MHz, 10 MHz, respectively. The measured results basically agree with the simulated ones and meet the requirement of CNSS terminal antennas.

1. INTRODUCTION

With the rapid development of navigation satellite systems, China is accelerating the development of its own navigation system called Compass Navigation Satellite System (CNSS for short) with location information and communication services [1]. Recently, its applications in civil and military domains have been rapidly developed to achieve fast, continuous and accurate positioning services. The communication function can be achieved by a dual-band terminal antenna which operates at L band (1616 ± 5 MHz, left-handed circular polarization) to send information and S band (2492 ± 5 MHz, right-handed circular polarization) to receive information [2–5]. Consequently, demand for dual-band dual-polarized and high-performance terminal antenna for CNSS has greatly increased. Microstrip patch antennas have narrow bandwidth typically 1–5% because of inherent constraints. When 3 dB axial ratio bandwidth and antenna gain are more than 20 MHz and 3 dB, we believe that this antenna meet the requirement of CNSS antenna.

Since the 1960s, spiral antennas have emerged as leading candidates for various commercial and military applications such as broadband satellite communication services and high-quality wireless communication systems. Moreover, planar spiral antennas have been extensively used in many fields due to their characteristics of broad bandwidth, circular polarization and small physical size. Circularly polarized antennas are more attractive because linearly polarized receiving antenna can only receive part or none of the circularly polarized signal, which significantly lowers the antenna's efficiency [6, 7]. Consequently, many broadband and dual-band circular-polarized planar spiral antennas have been

Received 10 March 2014, Accepted 27 April 2014, Scheduled 3 May 2014

* Corresponding author: Hangying Yuan (yhy1872937@126.com).

[1] College of Science, Air Force Engineering University, Xi'an 710051, China. [2] Electronic Materials Research Laboratory, Key Laboratory of the Ministry of Education, Xi'an Jiaotong University, Xi'an 710049, China.

reported [8–10]. In [11], a single-arm spiral antenna is presented which can achieve dual-sense circular polarization by feeding at either the inner or outer spiral end.

Limited by fabrication ability of multi-layer antenna [12] and inspired by the irreplaceable advantages of spiral structure, in this paper, we present a dual-band dual-circular-polarized planar spiral antenna for CNSS. The dual-band and CP radiation characteristics are realized by inserting a large spiral slot and a stepped microstrip feedline. The inner embedded spiral slot is used to improve the axial ratio bandwidth. By adjusting the width and length of the microstrip feedline, we can also improve the matching for two bands.

This paper is organized as follows. In Section 2, the geometry of the proposed antenna is clearly described. The simulated and measured results at two frequencies are given in Section 3. Finally, conclusion is provided in Section 4.

2. ANTENNA DESIGN

The geometry of the proposed antenna is given in Figure 1. This antenna consists of two spiral slots. The larger slot is used to achieve dual-band dual polarization performance and the smaller one to improve matching and 3 dB axial ratio (AR) bandwidth for the low frequency band. Two spiral slots are approximately one and a quarter turns long, and the radius sequentially increases with movement of the origin point each quarter turn. For the larger slot, the starting values are outer radius R_1 and origin O_1. The second quadrant has an outer radius R_2 and origin O_2. The 3rd, 4th and subsequent quadrants have radii R_3, R_4 and R_5 with origins O_3, O_4 and O_1, respectively. The larger slot maintains the same width W_1. For the smaller slot, the starting values are outer radius L_1 and origin O_3. The subsequent quadrants have radii L_2, L_3, L_4 and L_5 with origins O_4, O_1, O_2 and O_3, respectively. The smaller slot maintains the same width W_2.

A low-cost substrate with $\varepsilon_r = 2.2$, $\tan\delta = 0.0009$ and $h = 0.787\,\text{mm}$ was chosen. A parametric study was carried out using High Frequency Structure Simulator (HFSS) to achieve optimal performances. By the optimization, the geometric dimensions of the proposed antenna are as follows: $a = 100\,\text{mm}$, $R_1 = 23\,\text{mm}$, $R_2 = 25\,\text{mm}$, $R_3 = 27\,\text{mm}$, $R_4 = 29\,\text{mm}$, $R_5 = 31\,\text{mm}$, $L_1 = 10.5\,\text{mm}$, $L_2 = 12.5\,\text{mm}$, $L_3 = 14.5\,\text{mm}$, $L_4 = 16.5\,\text{mm}$, $L_5 = 18.5\,\text{mm}$, $L_{s1} = 22\,\text{mm}$, $L_{s2} = 22\,\text{mm}$, $W_{s1} = 1.2\,\text{mm}$, $W_{s2} = 2.5\,\text{mm}$. The $50\,\Omega$ microstrip feedline ($W_{s2} = 2.5\,\text{mm}$) is stepped to $W_{s1} = 1.2\,\text{mm}$ for good matching to the higher impedance slot. Meanwhile, subsequent radii increase by 2 mm per quarter circle to provide best axial ratio and matching.

An experiment was carried out to verify our design. Figure 2 shows the prototype of the proposed microstrip antenna.

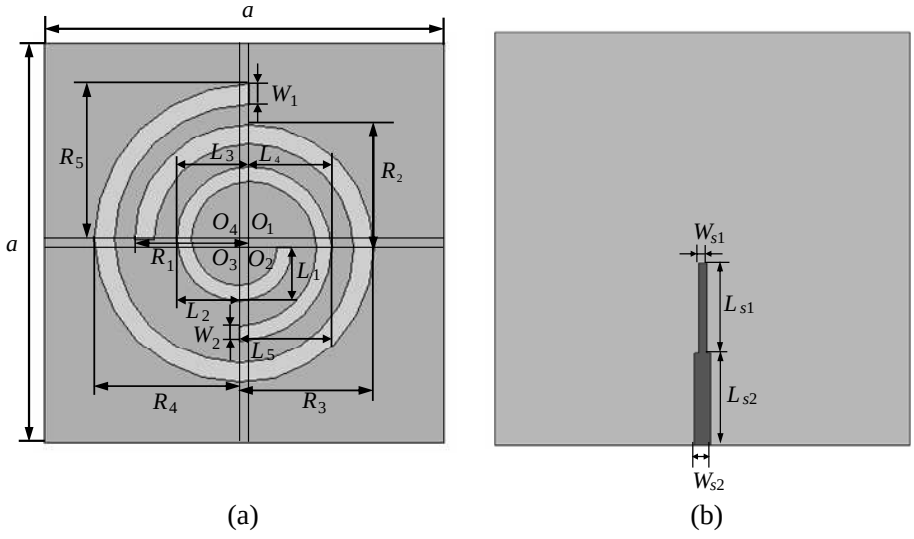

Figure 1. Geometry of the proposed antenna. (a) Top view. (b) Bottom view.

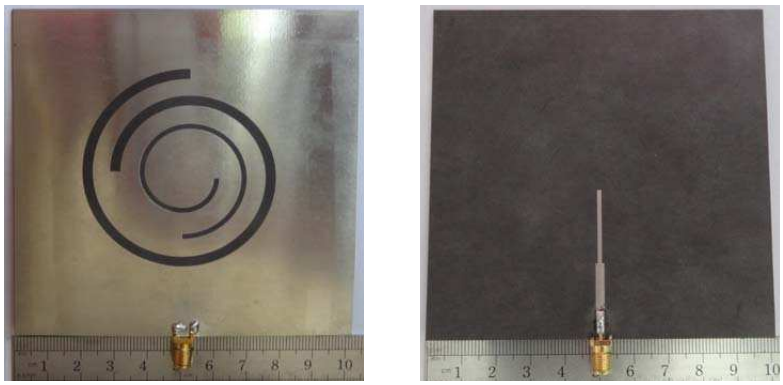

(a) (b)

Figure 2. Prototype of the proposed antenna. (a) Top view. (b) Bottom view.

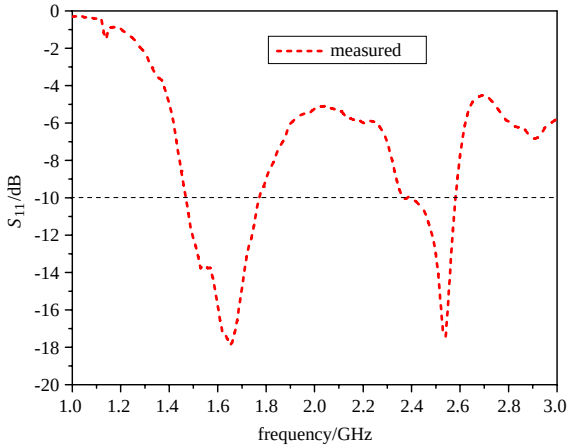

Figure 3. Simulated and measured reflection coefficient at 1–3 GHz.

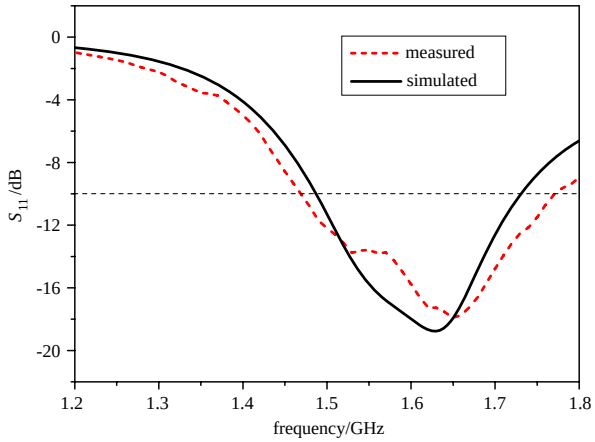

Figure 4. Simulated and measured reflection coefficient at 1.616 GHz.

3. SIMULATED AND MEASURED RESULTS

We used the full wave simulation software High Frequency Structure Simulator (HFSS) version 12.0 to calculate its performances. The measured reflection coefficient (S_{11}) at 1–3 GHz is given in Figure 3. From Figure 3, we can see that this antenna achieves good dual-band characteristic.

Comparison of the simulated and measured impedance bandwidths at 1.616 GHz is given in Figure 4. The solid line is the curve of simulated result, while the dashed line is the curve of measured result. From Figure 4, we can see that at L-band, the simulated impedance bandwidth is 242 MHz, and the $S_{11} < -10$ dB band is from 1.488 GHz to 1.730 GHz. Meanwhile, the measured impedance bandwidth is 300 MHz, and the $S_{11} < -10$ dB band is from 1.47 GHz to 1.77 GHz. The measured impedance bandwidth is 58 MHz larger than the simulated impedance bandwidth.

The simulated and measured impedance bandwidth at 2.492 GHz is given in Figure 5. The solid line is the curve of simulated result, while the dashed line is the curve of measured result. From Figure 5, we can see that at S-band, the simulated impedance bandwidth is 180 MHz, and the $S_{11} < -10$ dB band is from 2.415 GHz to 2.595 GHz. Meanwhile, the measured impedance bandwidth is 210 MHz, and the $S_{11} < -10$ dB band is from 2.37 GHz to 2.58 GHz. The measured impedance bandwidth is 30 MHz larger than the simulated impedance bandwidth.

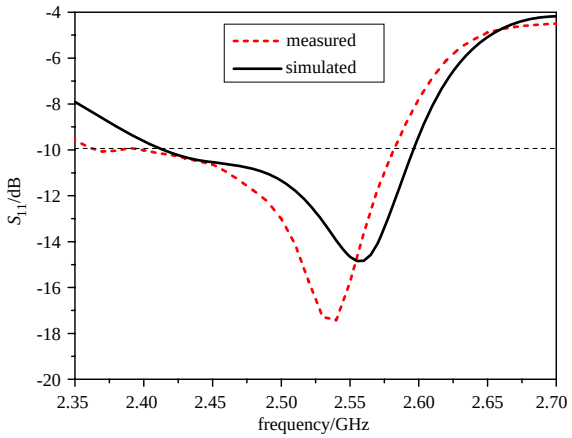

Figure 5. Simulated and measured reflection coefficient at 2.492 GHz.

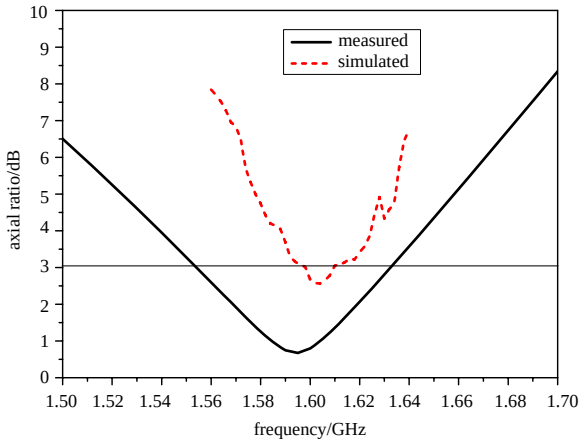

Figure 6. Simulated and measured axial ratio at 1.616 GHz.

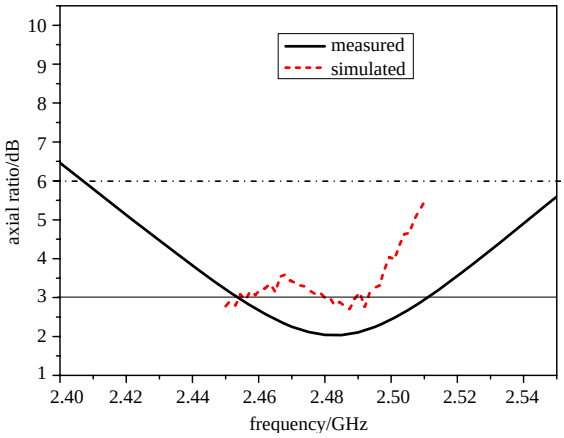

Figure 7. Simulated and measured axial ratio at 2.492 GHz.

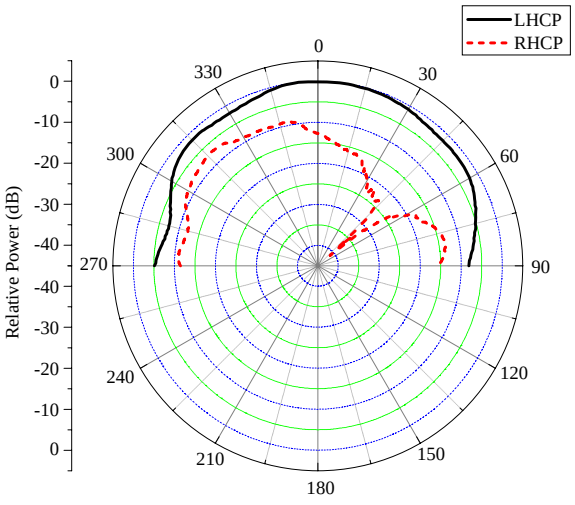

Figure 8. The measured LHCP and RHCP radiation patterns of the antenna at 1.616 GHz.

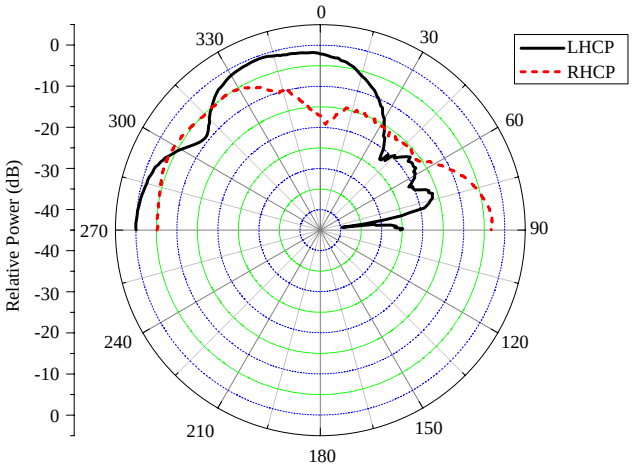

Figure 9. The measured RHCP and LHCP radiation patterns of the antenna at 2.492 GHz.

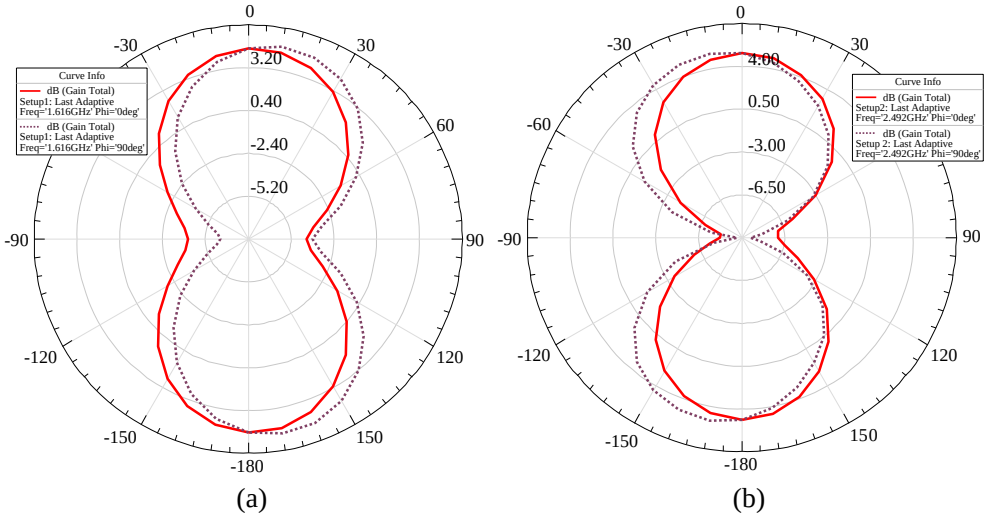

Figure 10. The simulated antenna gain at L- and S-bands. (a) At L-band. (b) At S-band.

Figure 6 shows the simulated and measured axial ratio at 1.616 GHz. The solid line is the curve of simulated result, while the dashed line is the curve of measured result. We can see that at L-band, the simulated axial ratio bandwidth is 79 MHz, and the AR < 3 dB band is from 1.553 GHz to 1.632 GHz. Meanwhile, the measured axial ratio bandwidth is 14 MHz.

Figure 7 shows the simulated and measured axial ratio at 2.492 GHz. The solid line is the curve of simulated result, while the dashed line is the curve of measured result. We can see that at S-band, the simulated axial ratio bandwidth is 58 MHz, and the AR < 3 dB band is from 2.453 GHz to 2.511 GHz. Meanwhile, the measured axial ratio bandwidth is 10 MHz.

Figure 8 shows the measured LHCP and RHCP radiation patterns of the proposed antenna at 1.616 GHz. The solid line is the LHCP curve, while the dashed line is the RHCP curve. It is obvious that this antenna achieves good left-handed circularly polarized characteristic at L-band.

Figure 9 shows the measured RHCP and LHCP radiation patterns of the proposed antenna at 2.492 GHz. The solid line is the RHCP curve, while the dashed line is the LHCP curve. We can see that this antenna achieves right-handed circularly polarized characteristic at S-band.

Due to the lack of normative horn antennas at L- and S-bands, it is difficult for us to measure the gain of this antenna. The simulated antenna gain at L-band is 4.92 dB, and the simulated gain at S-band is 5.25 dB. Figure 10 shows the simulated antenna gain at L- and S-bands.

4. CONCLUSION

We present a dual-band dual-polarized spiral-slot microstrip antenna capable of simultaneously sending LHCP L-signals and receiving RHCP S-signals of CNSS. The measured results agree with the simulated ones and meet the requirement of CNSS terminal antennas. The circular polarization characteristic is very sensitive to fabrication precision. We can scale and re-optimize this structure to provide a compact and high performance for many other separate frequency sets of interest.

ACKNOWLEDGMENT

This work was supported in part by the National Science Foundation for Post-doctoral Scientists of China under Grant Nos. 2013M532131, 2013M532221, and in part by the National Natural Science Foundation of China under Grants No. 61302023.

REFERENCES

1. Liu, W. Z., Y. Huang, and X. P. Zhang, "A compact tri-band antenna switch module for compass satellite positioning application," *IEEE Microwave Conference Proceedings (APMC)*, 869–871, 2013.
2. Zhang, P. P., H. Wang, and Y. Wang, "Investigations of compact tri-band antenna for CNSS application," *IEEE Microwave Conference Proceedings (APMC)*, 1100–1102, 2013.
3. Tian, X. Q., S. B. Liu, Y. S. Wei, and X. Y. Zhang, "Circularly polarized microstrip antenna with slots for Beidou (COMPASS) Navigation System," *Proceedings of International Symposium on Signals, Systems and Electronics, ISSSE*, Vol. 2, 1–3, 2010.
4. Liao, W., Q.-X. Chu, and S. Du, "Tri-band circularly polarized stacked microstrip antenna for GPS and CNSS applications," *ICMMT Proceedings*, 252–255, 2010.
5. Wu, S.-Q., S.-B. Liu, and Z. Guo, "Coaxial probe-fed circularly polarized microstrip antenna for Beidou RDSS applications," *ICMMT Proceedings*, 297–299, 2010.
6. Heidari, A. A., M. Heyrani, and M. Nakhkash, "A dual-band circularly polarized stub loaded microstrip patch antenna for GPS applications," *Progress In Electromagnetics Research*, Vol. 92, 195–208, 2009.
7. Yang, S. L. S., K. F. Lee, and A. A. Kishk, "Design and study of wideband single feed circularly polarized microstrip antennas," *Progress In Electromagnetics Research*, Vol. 80, 45–61, 2008.
8. Muller, D. J. and K. Sarabandi, "Design and analysis of a 3-arm spiral antenna," *IEEE Transaction on Antennas and Propagation*, Vol. 55, No. 2, 258–266, 2007.
9. Stutzke, N. A. and D. S. Filipovic, "Four-arm 2nd-mode slot spiral antenna with simple single-port feed," *IEEE Antennas Wireless Propagation Letters*, Vol. 4, 213–216, 2005.
10. Laheurte, J. M., "Dual-frequency circularly polarized antennas based on stacked monofilar square spirals," *IEEE Transactions on Antennas and Propagation*, Vol. 51, No. 3, 488–492, 2003.
11. Jung, C. W., B. A. Cetiner, and F. De Flaviis, "A single-arm circular spiral antenna with inner/outer feed circuitry for changing polarization and beam characteristics," *IEEE Antennas and Propagation Society International Symposium Proceedings*, 474–477, 2003.
12. Yuan, H. Y., J. Q. Zhang, S. B. Qu, H. Zhou, J. F. Wang, H. Ma, and Z. Xu, "Dual-band dual-polarized microstrip antenna for compass navigation satellite system," *Progress In Electromagnetics Research C*, Vol. 30, 213–223, 2012.